Combination treatment of adipose-derived stem cells and adiponectin attenuates pulmonary arterial hypertension in rats by inhibiting pulmonary arterial smooth muscle cell proliferation and regulating the AMPK/BMP/Smad pathway

LI LUO, WUHONG ZHENG, GUILI LIAN, HUANING CHEN, LING LI, CHANGSHENG XU and LIANGDI XIE

Fujian Hypertension Research Institute, The First Affiliated Hospital of Fujian Medical University, Fuzhou, Fujian 350005, P.R. China

Received October 21, 2016; Accepted October 12, 2017

DOI: 10.3892/ijmm.2017.3226

Abstract. The present study aimed to assess the effects of therapy with adiponectin (APN) gene-modified adipose-derived stem cells (ADSCs) on pulmonary arterial hypertension (PAH) in rats and the underlying cellular and molecular mechanisms. ADSCs were successfully isolated from the rats and characterized. ADSCs were effectively infected with the green fluorescent protein (GFP)-empty (ADSCs-V) or the APN-GFP (ADSCs-APN) lentivirus and the APN expression was evaluated by ELISA. Sprague-Dawley rats were administered monocrotaline (MCT) to develop PAH. The rats were treated with MCT, ADSCs, ADSCs-V and ADSCs-APN. Then ADSCs-APN in the lung were investigated by confocal laser scanning microscopy and western blot analysis. Engrafted ADSCs in the lung were located around the vessels. Mean pulmonary arterial pressure (mPAP) and the right ventricular hypertrophy index (RVHI) in the ADSCs-APN-treated mice were significantly decreased as compared with the ADSCs and ADSCs-V treatments. Pulmonary vascular remodeling was assessed. Right ventricular (RV) function was evaluated by echocardiography. We found that pulmonary vascular remodeling and the parameters of RV function were extensively improved after ADSCs-APN treatment when compared with ADSCs and ADSCs-V treatment. Pulmonary artery smooth muscle cells (PASMCs) were isolated from the PAH rats. The antiproliferative effect of APN on PASMCs was assayed by Cell Counting Kit-8. The influence of APN and specific inhibitors on the levels of bone morphogenetic protein (BMP), adenosine monophosphate activated protein kinase (AMPK), and small mothers against decapentaplegia (Smad) pathways was detected by western blot analysis. We found that APN suppressed the proliferation of PASMCs isolated from the PAH rats by regulating the AMPK/BMP/Smad pathway. This effect was weakened by addition of the AMPK inhibitor (compound C) and BMP2 inhibitor (noggin). Therefore, combination treatment with ADSCs and APN effectively attenuated PAH in rats by inhibiting PASMC proliferation and regulating the AMPK/BMP/Smad pathway.

Introduction

Pulmonary arterial hypertension (PAH) aggressively threatens human health with high morbidity and mortality due to its diverse etiologies. Unfortunately, current strategies are ineffective to prevent and cure PAH. In recent years, multipotent stem cells, such as adipose-derived stem cells (ADSCs), bone marrow mesenchymal stem cells, and endothelial progenitor cells (EPCs), have been employed as a promising strategy for PAH therapy (1-3). These studies have revealed that stem cells play crucial roles in the prevention and treatment of PAH by repairing endothelial cells and angiogenesis and inhibiting pulmonary arterial remodeling (1-3). Moreover, our previous study also demonstrated that ADSCs attenuated PAH and ameliorated pulmonary arterial remodeling in rats with PAH (4).

Generally, due to the complex pathogenesis of PAH, cell transplantation alone cannot solve all the issues. Cell-based gene therapy has been found to be effective in preclinical models of PAH (5,6). Several studies have indicated that prepro calcitonin gene-related peptide (CGRP)-transfected EPCs, vascular endothelial growth factor-transfected EPCs, and hypoxia inducible factor 1α-transfected EPCs could effectively attenuate PAH and reverse pulmonary vascular remodeling (7-9). A PHACeT clinical trial reported that short-term hemodynamic improvement and the associated long-term benefits in functional and quality of life were evidenced in patients with PAH by delivering endothelial NO-synthase (eNOS) gene-enhanced EPCs (10). Therefore, combination treatment is more effective than single stem cell transplantation. Stem cell transplantation combined with gene therapy may be an extremely promising treatment for PAH.

Correspondence to: Professor Liangdi Xie, Fujian Hypertension Research Institute, The First Affiliated Hospital of Fujian Medical University, Fuzhou, Fujian 350005, P.R. China
E-mail: ldxie@hotmail.com

Key words: adiponectin, adipose-derived stem cells, pulmonary arterial hypertension, gene therapy, pulmonary arterial smooth muscle cells, AMPK/BMP/Smad pathway

Adiponectin (APN), a 30-kDa multimeric protein produced by fat cells, has multiple biological functions including anti-oxidation, anti-atherosclerosis, anti-inflammation and anti-proliferation activity (11-13). It can protect blood vessels through various mechanisms. APN-deficient mice ($APN^{-/-}$) suffer from PAH accompanied by infiltration of proinflammatory cells and overexpression of endothelial E-selectin (14-16). Nakagawa *et al* reported that upregulation of APN significantly suppressed pulmonary arterial wall thickening and right ventricular (RV) hypertrophy induced by chronic hypoxia in mice (17). Nevertheless, APN treatment for PAH and the underlying mechanisms have not been well probed.

Abnormal proliferation of pulmonary artery smooth muscle cells (PASMCs) is a common pathologic feature of pathological pulmonary vasculature (18). Bone morphogenetic protein (BMP) receptor type 2 (BMPR2) is a member of the transforming growth factor-β (TGF-β) receptor superfamily. Its mutations were confirmed in the majority of patients with heritable PAH (19,20). In PAH models induced by monocrotaline (MCT) and hypoxia, BMPR2 expression was downregulated and the BMP signaling pathway was disordered (21,22). Enhancement of the BMPR2 pathway could inhibit the proliferation and promote the apoptosis of PASMCs (23), which may be ultilized for the treatment of pathological pulmonary vasculature.

Therefore, this study aimed to probe the therapeutic efficacy of APN gene-modified ADSCs for PAH in rats and elucidate the underlying cellular and molecular mechanisms.

Materials and methods

Materials and animals. Adenosine monophosphate activated protein kinase (AMPK) inhibitor compound C (CC) was purchased from Merck (Darmstadt, Germany). APN, rabbit anti-α-smooth muscle actin (α-SMA) antibody (ab5694), rabbit anti-AMPK antibody (ab32047), and mouse anti-BMP2 antibody (ab6285) were obtained from Abcam (Cambridge, UK). BCA protein assay kit and rabbit anti-Smad1/5/8/9 antibody (PA1-41238) were from Pierce (Rockford, IL, USA). BMP2 inhibitor noggin was purchased from R&D Systems Inc. (Minneapolis, MN, USA). Cell Counting Kit-8 (CCK-8) was from Dojindo (Kumamoto, Japan). CD29 (102205), CD45 (202205) and CD90 (202517) antibodies were from BioLegend (San Diego, CA, USA). CD31 antibody (ab119339), rat APN enzyme-linked immunosorbent assay (ELISA) kit and adiponectin antibody were from Abcam. Collagenase type I and MCT were purchased from Sigma-Aldrich (St. Louis, MO, USA). 3,3'-Diaminobenzidine tetrahydrochloride hydrate (DAB) was from Zhongshan Goldenbridge (Beijing, China). 4',6-Diamidino-2-phenylindole (DAPI) was obtained from Beyotime Institute of Biotechnology (Jiangsu, China). Dulbecco's modified Eagle's medium (DMEM), DMEM-F12 medium, and fetal bovine serum (FBS) were obtained from HyClone (Logan, UT, USA). Enhanced chemiluminescent (ECL) reagent was from Amersham (Piscataway, NJ, USA). Goat anti-rabbit IgG was obtained from ZSGB-Bio (Beijing, China). Optimal cutting temperature compound (OCT) was obtained from Miles Scientific (Naperville, IL, USA). Rabbit anti-p-AMPK (2535S) and rabbit anti-p-Smad1/5/8/9 (9511S) antibodies were purchased from Cell Signaling Technology (Danvers, CO, USA). Rabbit anti-β-actin (sc-10731) and CD34 (sc-65261) antibodies were obtained from Santa Cruz Biotechnology, Inc. (Dallas, TX, USA). SD rat ADSC functional identification kit was bought from Cyagen Biosciences, Inc. (Guangdong, China).

Male Sprague-Dawley (SD) rats (8-weeks of age) were obtained from Slaccas Co. Ltd. (Shanghai, China) (certificate no. 20120003). All animals were raised with food and water *ad libitum*. The study protocol was reviewed and approved by the Institutional Animal Care and Use Committee, The First Affiliated Hospital of Fujian Medical University, China and was in accordance with the guidelines established by the Chinese Council of Animal Care.

Isolation and characterization of ADSCs. ADSCs were isolated from the rats as described in our previous study (4). Briefly, bilateral inguinal subcutaneous adipose tissue was excised, minced, and digested with 0.1% collagenase type I for 60 min at 37˚C. The mixture containing the ADSC fraction was filtered through a mesh and centrifuged for 10 min at 1,000 x g. The resultant pellet was resuspended and cultured in DMEM-F12 media containing 15% FBS at 37˚C in 5% CO_2. After 3 to 4 days, the culture medium was completely changed. All cells were cultured for another 14 days with a change of the culture media every 3 days. The multipotency of ADSCs was assessed via adipogenic and osteogenic differentiation assays by using the SD rat ADSC functional identification kit according to the manufacturer's instructions for use. ADSCs were incubated with CD31, CD29, CD34, CD45 and CD90 antibodies and then assayed by using flow cytometry (BD FACSCalibur; BD Biosciences, Franklin Lakes, NJ, USA).

Infection of ADSCs with the APN lentiviral vector. After being cultured for 14 days, ADSCs were infected with green fluorescent protein (GFP)-empty (ADSCs-V) or APN-expressing lentiviral vector (ADSCs-APN) at a multiplicity of infection (MOI) of 10. The GFP-empty lentivirus served as a negative control. Rat APN-GFP cDNA was cloned in the GV287 vector from GenePharma Co, Ltd. (Shanghai, China). Primers for rat APN were forward, ACTCAGCATTCAGCGTAGGG and reverse, CGTCGCCGTCCAGCTCGACCAG. After incubation for 12 h, the medium was replaced by fresh DMEM and the cells were cultured for another 72 h. Supernatants were collected for the quantification of APN protein using the rat APN ELISA kit according to the manufacturer's instruction for use. The absorbance was determined at 450 nm with a sensitivity of 1.5 ng/ml.

Animal treatments. Forty SD rats were randomly divided into five groups (n=8): normal control (Ctr), PAH, ADSCs, ADSCs infected with the GFP empty lentiviral vector (ADSCs-V), and APN-GFP gene-modified ADSCs (ADSCs-APN). Rats in the PAH, ADSCs, ADSCs-V and ADSCs-APN groups were intraperitoneally administered 40 mg/kg MCT, while those in the Ctr group were injected with an equal volume of saline. After 2 weeks, $1.0x10^6$ ADSCs, ADSCs infected with the GFP empty lentiviral vector, and APN-GFP gene-modified ADSCs were injected into the left jugular vein of the rats, respectively. Three weeks later, mean pulmonary arterial pressure (mPAP) was measured as described below. Then the rats

were euthanized, and the lung and heart tissues were collected for following analyses.

ADSCs-APN in the lung. To determine the location of the ADSCs in the lung, GFP-labeled ADSCs were evaluated by confocal laser scanning microscopy. The right upper lobe of the lung was dissected and washed with phosphate-buffered saline (PBS). The tissue was perfused with a mixture of formalin and OCT, embedded in OCT, and quickly frozen in liquid nitrogen. Then the frozen tissue was sectioned. Cryostat sections were fixed with formalin for 10 min and incubated with DAPI for 10 min. The sections were examined using FlowView software (V2.0c) on a confocal laser scanning microscope (FV1000) (both from Olympus, Tokyo, Japan) for determining the distribution of the GFP-labeled ADSCs in lung tissue. Images were captured in the XYZ scan mode from top to bottom of the section. GFP was excited at 488 nm and DAPI was excited at 405 nm.

The expression of APN in the lung was detected by western blot analysis. Lung tissue was homogenized and lysed in a protein extraction buffer containing the protease inhibitor phenylmethylsulfonyl fluoride. The protein concentration was determined using a BCA protein assay kit. Proteins were separated using 10% sodium dodecyl sulfate-polyacrylamide gel electrophoresis (SDS-PAGE), and then transferred to a polyvinylidene fluoride (PVDF) membrane. The membrane was incubated with the adiponectin antibody (1:1,000) and the subsequent secondary antibody. The membrane was analyzed on a gel imaging system (ChemiDoc™ XRS; Bio-Rad, Hercules, CA, USA). The optical densities of protein strips were evaluated with a Gel-Pro analyzer software (Media Cybernetics, Rockville, MD, USA).

Measurement of mPAP and RV hypertrophy index (RVHI). After treatments, rats were anesthetized with 10% chloral hydrate (400 mg/kg). mPAP was recorded as described previously (4,24). In brief, polyethylene micro-catheters (Chinese Peking Union Medical Physiology) were inserted into the pulmonary artery via the right external jugular vein and connected to a transducer. The mPAP data were collected and analyzed by Powerlab-ML221 (AD Instruments, New South Wales, Australia). RVHI was assessed by weighing the RV separately from the left ventricle (LV) with the septal wall (SW).

Pulmonary vascular remodeling analysis. Paraffin-embedded sections were prepared and stained with hematoxylin and eosin (H&E). Pulmonary arteriolae between 50 and 200 μm in external diameter (ED) were chosen for morphological analysis. Wall thickness (WT) and ED of the pulmonary arteries were measured using IPP 6.0 image analysis software (Media Cybernetics). The remodeling of pulmonary arterioles was calculated as WT% = 2 x WT/ED x100% (4,24). For immunohistochemical analysis, sections were incubated with α-SMA antibody at 4˚C overnight followed by the secondary antibody. Subsequently, they were incubated with DAB as a chromogen to visualize the antigen-antibody reaction and with hematoxylin for the counterstain of the nuclei.

RV function. The rats were sedated and laid in the supine position. Transthoracic echocardiography was performed using a GE Vivid-E9 ultrasound device (General Electric Co., Fairfield, CT, USA) with a 12.0 MHz linear array transducer. During the ultrasonic examination, the lead electrocardiogram was recorded and the heart rate (HR) was monitored. Pulmonary artery acceleration time (PAAT) was measured by a pulsed-wave Doppler in the parasternal short-axis view and defined as the time interval from onset to the maximal velocity of pulmonary artery forward flow. Since PAAT is HR-dependent, we corrected the PAAT using the revised formula PAAT/HR. Right ventricular WT (RVWT), right ventricular end systolic diameter (RVESD), and right ventricular end diastolic diameter (RVEED) were obtained from the apical 4-chamber view. Tricuspid annular plane systolic excursion (TAPSE) was measured by M-mode tracings. The echocardiographic parameters were analyzed with Echo software by a sonographer who was blinded to the hemodynamic and morphological data. Three representative cycles were conducted.

Prepartion of PASMCs. Pulmonary artery tissues were isolated from the rats in the PAH group. The pulmonary arteries were separated from the connective tissues, minced to a size of ~1x1 mm, placed into a dish, and incubated with DMEM supplemented with 15% FBS. PASMCs were identified as having a smooth muscle phenotype by positive immunofluorescence with the anti-α-SMA rabbit antibody. After 3-5 cell passages, the cells were used for the following experiments.

Cell proliferation assay. The anti-proliferative effect of APN on PASMCs was evaluated by the CCK-8 assay. PASMCs ($2x10^4$ cells/well) were seeded in 96-well plates containing 100 μl DMEM supplemented with 15% FBS per each well and cultured for 24 h. Cells were washed twice with PBS. Subsequently, cells were starved for 24 h in serum-free medium and treated with 200 ng/ml noggin and/or 10 μg/ml APN. Cells without any treatments served as the control. Following a 24-h incubation, 10 μl of CCK-8 was added to each well for 2 h. The plates were submitted to a microplate reader (Bio-Rad 550; Leading Biological Technology Co. Ltd., Shanghai, China) for absorbance determination at 450 nm.

APN intervention. To investigate the effect of APN on the expression of BMP2 in PASMCs, the cells ($1x10^5$/ml) were seeded in 6-well plates. After confluence reached ~70-80%, the cells were exposed to different concentrations (0, 1.0, 5.0, 10.0 and 20.0 μg/ml) of APN for 1 h. In addition, cells were exposed to APN at 10 μg/ml for 0, 5, 15 and 30 min, 1, 6, 24 and 36 h (15,25). The expression of BMP2 was detected by western blot analysis. To probe the effect of APN on the expression of Smad, phosphorylated (p)-Smad (p-Smad), AMPK, and p-AMPK in PASMCs, before exposure to APN (10 μg/ml), the cells were starved in serum-free medium for 24 h, washed twice with PBS, and treated with 200 ng/ml BMP2 inhibitor noggin and AMPK inhibitor CC for 4 h, respectively.

Western blot analysis. After treatments, PASMCs were lysed with ice-cold RIPA lysis buffer for 10 min and centrifuged for 15 min at 12,000 x g and 4˚C. The supernatants were collected. The protein concentration was determined by using a BCA protein assay kit. Proteins were separated on 6 or 10% SDS-PAGE and then transferred to a PVDF membrane. The membrane was

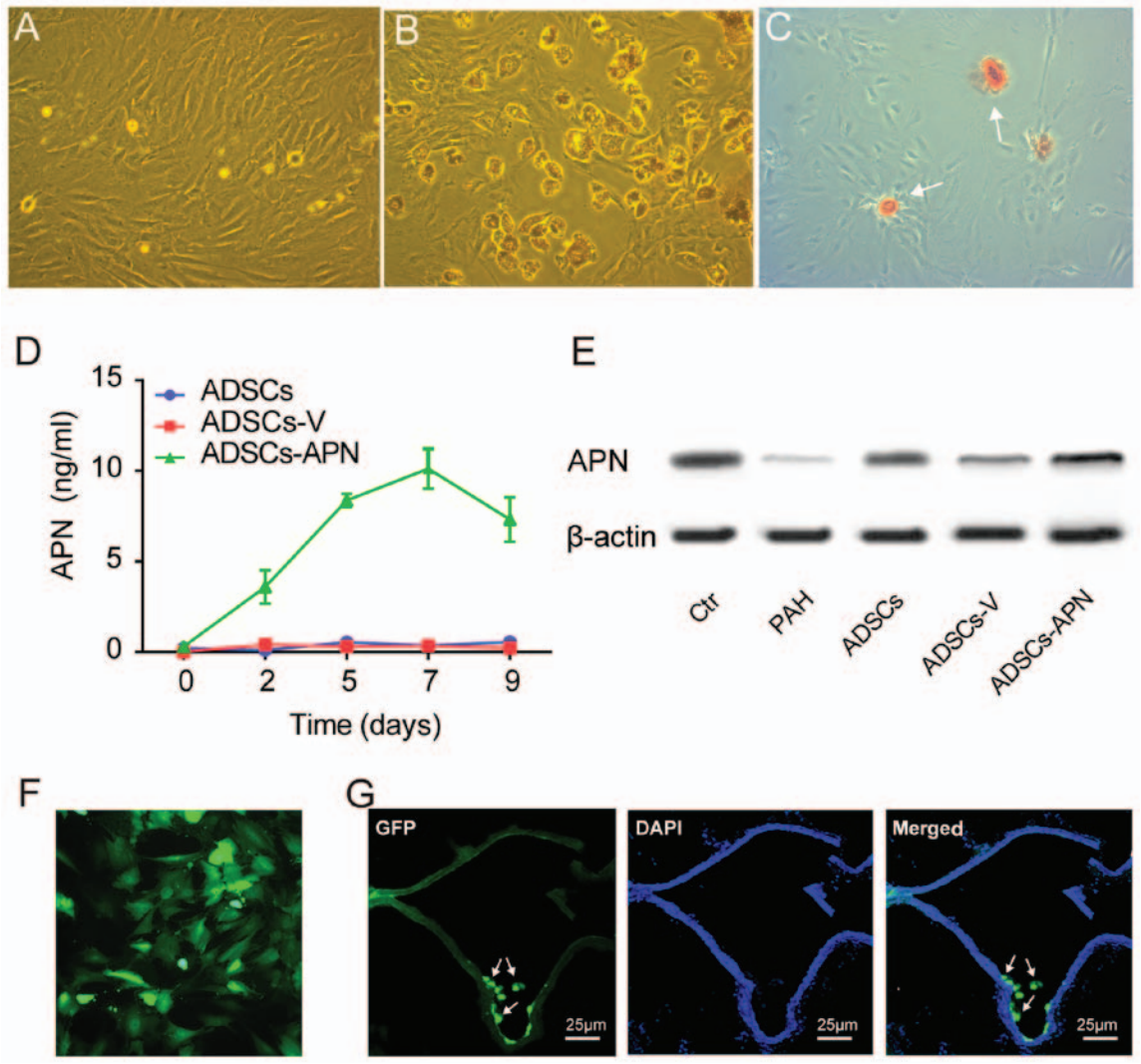

Figure 1. Adipose-derived stem cell (ADSC) characterization and adiponectin (APN) expression. (A) ADSCs isolated from rats had spindle-shaped and fibroblast-like morphological features. (B) After adipogenic induction, intracellular lipid accumulation was observed by Oil Red O staining. (C) After osteogenic induction, extracellular matrix calcification was detected by Alizarin red staining. (D) APN expression in the various groups. (E) APN protein expression in the lung was evaluated by western blot analysis. (F) Representative fluorescence microscopy image of green fluorescent protein (GFP)-expressing ADSCs *in vitro* (green). (G) Distribution of intravenously administered ADSCs in lung tissue. GFP-expressing rat ADSCs (green) were incorporated into walls of pulmonary vascular beds. Nuclei were stained by DAPI. Scale bars, 25 μm.

blocked with 5% nonfat milk for 1 h at room temperature and then incubated with rabbit anti-p-AMPK (1:1,000), rabbit anti-AMPK (1:1500), mouse anti-BMP2 (1:1,000), rabbit anti-p-Smad1/5/8/9 (1:500), rabbit anti-Smad1/5/8/9 (1:1,000), and rabbit anti-β-actin (1:1,000) antibodies at 4˚C overnight. After washing, the membrane was incubated with horseradish peroxidase (HRP)-conjugated secondary antibody (X-Y Biotechnology Co., Ltd., Shanghai, China) in TBS-T for 1 h and then incubated with ECL reagent at room temperature. The membrane was analyzed on a gel imaging system (ChemiDoc™ XRS; Bio-Rad). The optical densities of protein strips were assessed with a Gel-Pro analyzer software (Media Cybernetics).

Statistical analysis. Data are expressed as mean ± standard error of the mean (SEM). Comparisons among groups were made using one-way ANOVA followed by the Newman-Keuls test for post hoc testing on SPSS 20.0 software. A significant difference was defined as $P<0.05$.

Results

Characterization of ADSCs and transfection of APN into ADSCs. ADSCs isolated from rats exhibited spindle-shape and fibroblast-like morphological features (Fig. 1A). ADSCs were able to differentiate into adipogenic and osteogenic cells after appropriate induction (Fig. 1B and C). Flow cytometry showed that these ADSCs were positive for mesenchymal stem cell markers CD90 (97.9%) and CD29 (87.6%), but negative for hematopoietic/endothelial cell markers CD45 (6.2%), CD31 (0.9%) and CD34 (37.9%) (data not shown).

After transfection of the GFP empty vector (ADSCs-V) or APN-GFP vector (ADSCs-APN) into ADSCs, the APN concentration in the ADSC supernatant was measured by ELISA for determining the secretion rate of APN. We found that the APN concentration was invariably not elevated in the ADSCs and ADSCs-V groups (Fig. 1D). However, in the ADSCs-APN group, the APN concentration began to increase

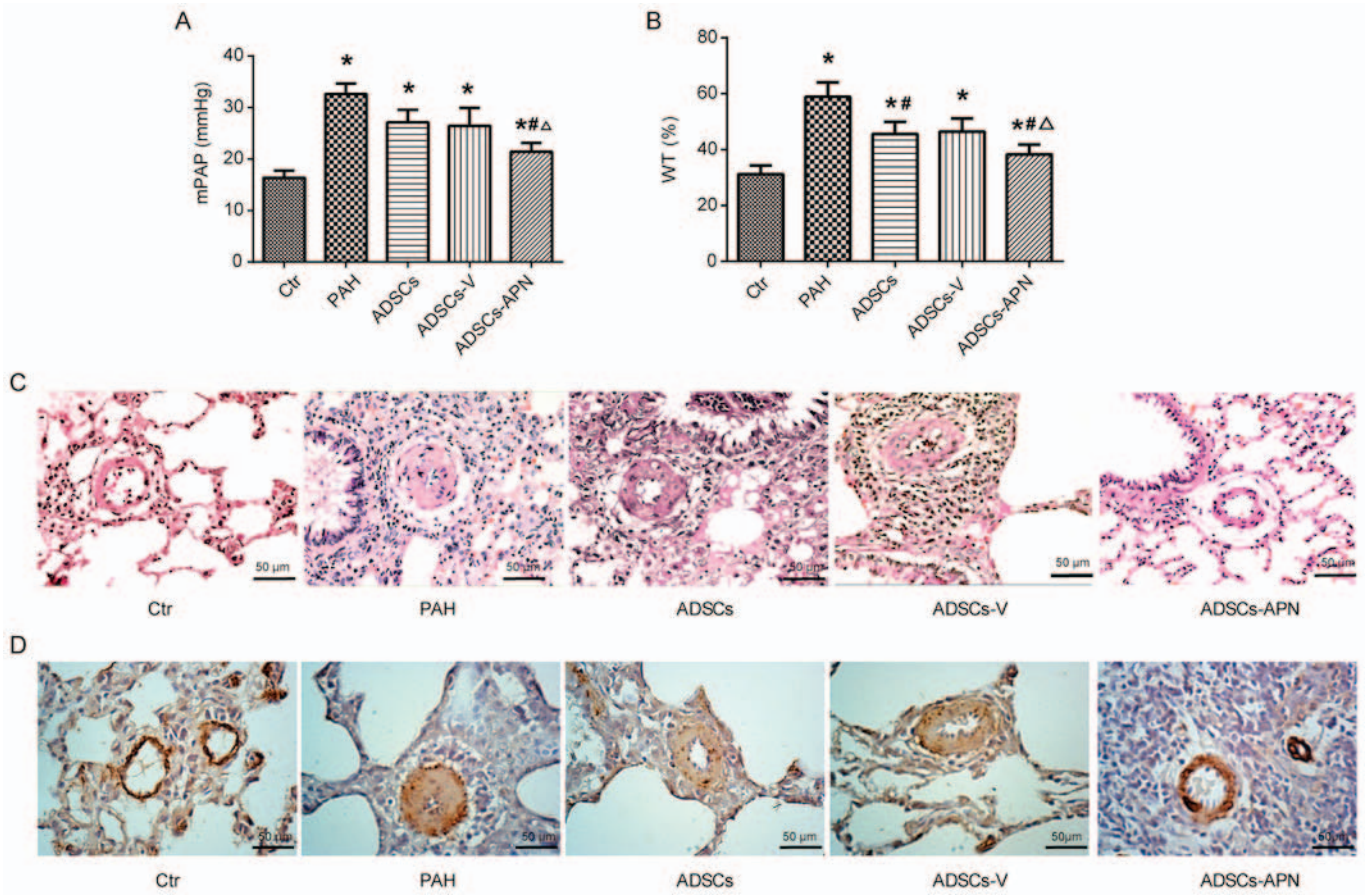

Figure 2. Effect of cell-based gene transfer on hemodynamic parameters and pulmonary vascular remodeling in the rats with pulmonary arterial hypertension (PAH). (A) Mean pulmonary arterial pressure (mPAP). (B) Wall to lumen thickness (WT%) in the Ctr, PAH, adipose-derived stem cells (ADSCs), ADSCs-V and ADSCs-adiponectin (APN) groups. *P<0.05 vs. Ctr group; #P<0.05 vs. PAH group; △P<0.05 vs. ADSCs group. (C) Representative pulmonary arteries with H&E staining. Scale bars, 50 μm. (D) Representative pulmonary arteries immunostained with α-smooth muscle actin (α-SMA) antibody. Scale bars, 50 μm. .

2 days after transfection and it reached the peak value on day 7.

ADSCs-APN in the lung. Western blot analysis was used to measure APN protein expression in the lung of rats after various treatments (Fig. 1E). It was demonstrated that expression of APN protein was obviously increased after ADSCs-APN transplantation (ADSCs-APN group) as compared with levels in the ADSCs and ADSCs-V groups. The location of GFP in ADSCs was evaluated by fluorescence microscopy (Fig. 1F). Twenty-four hours after APN gene transfection into ADSCs, the green fluorescence of GFP was observed within the cells and GFP was active after several passages. The frozen section with double fluorescence analysis was employed to evaluate the location of ADSCs-APN in the lung of rats (Fig. 1G). Results revealed that the green fluorescene of APN-GFP and the blue fluorescence of the cell nuclei were merged, suggesting the engraftment of ADSCs-APN across lung tissues of rats. The blue nuclei outlined the vascular wall and the green ADSCs were located around the vessels.

ADSCs-APN attenuate PAH. The mPAP results are depicted in Fig. 2A. In the Ctr group, mPAP was 16.38±0.91 mmHg. After MCT administration, PAH was well established with the mPAP of 32.62±1.77 mmHg. Compared to the PAH group, moderate decreases in mPAP were noted in the ADSCs and ADSCs-V groups with 27.11±2.12 and 26.44±2.91 mmHg, respectively. Notably, although the mPAP in the ADSCs-APN group (21.44±0.89 mmHg) was still significantly higher than that in the Ctr group, it was effectively reduced in comparison with the ADSCs and ADSCs-V groups (P<0.05). These results indicated that ADSCs-APN rather than ADSCs and ADSCs-V were capable of strongly attenuating PAH.

ADSCs-APN reverse pulmonary vascular remodeling. To determine the effect of ADSCs-APN on vascular remodeling, the WT of the pulmonary arteriolae in the rats was examined (Fig. 2B and C). Compared to the Ctr group, the WT% was markedly elevated in the PAH group (P<0.05), suggesting the progression of wall thickening in the pulmonary arterioles. However, the WT% in both the ADSCs and ADSCs-V groups was significantly lower than that in the PAH group (P<0.05). The WT% was further significantly reduced in the ADSCs-APN group as compared with the ADSCs and ADSCs-V groups (P<0.05), suggesting that ADSCs-APN transplantation further prevented arteriolar wall thickening.

α-SMA is a positive marker for smooth muscle cells (SMCs). The proliferation of pulmonary arterioles was evaluated by α-SMA expression analysis. Morphometric immunostaining of lung sections demonstrated that α-SMA

Table I. Echocardiographic parameters of the PAH rats after various treatments.

	Ctr	PAH	ADSCs	ADSCs-V	APN-ADSCs
TAPSE (mm)	2.87±0.23	1.48±0.10[a]	1.97±0.13[a,b]	1.87±0.08[a,b]	2.43±0.07[a,b,c]
RVEDD (mm)	2.55±0.18	4.23±0.58[a]	3.67±0.58[a]	3.70±0.32[a]	3.71±0.32[a]
RVESD (mm)	2.36±0.23	3.11±0.22[a]	2.68±0.53	2.72±0.18	2.84±0.44
RVWT (mm)	2.41±0.26	2.94±0.23[a]	2.68±0.27	2.69±0.29	2.68±0.27
PAAT/HR	0.25±0.02	0.14±0.02[a]	0.18±0.02[a,b]	0.18±0.02[a,b]	0.22±0.02[a,b,c]

[a]P<0.05 vs. Ctr group; [b]P<0.05 vs. PAH group; [c]P<0.05 vs. ADSC group. PAH, pulmonary arterial hypertension; ADSCs, adipose-derived stem cells; APN, adiponectin; TAPSE, tricuspid annular plane systolic excursion; RVEDD, right ventricular end diastolic diameter; RVESD, right ventricular end systolic diameter; RVWT, right ventricular wall thickness; PAAT, pulmonary artery acceleration time; HR, heart rate.

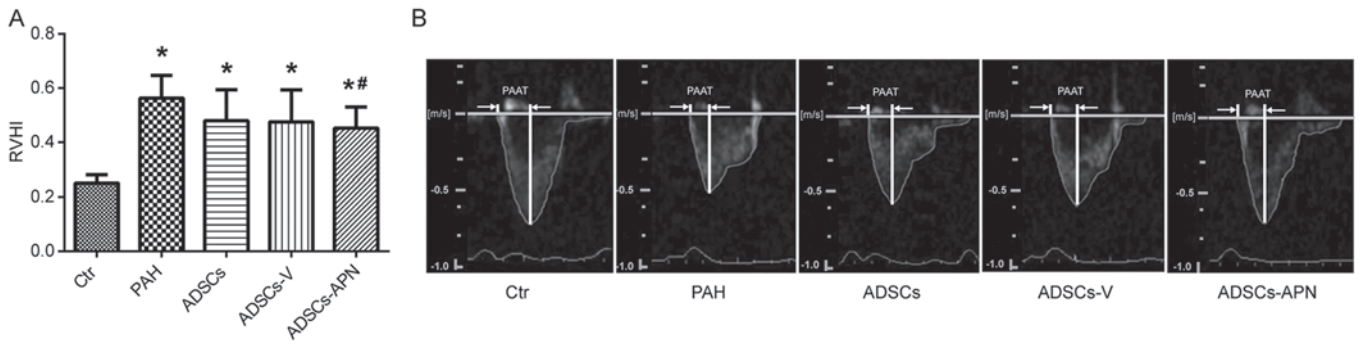

Figure 3. Effect of cell-based gene transfer on right ventricle function. (A) Index of right ventricular hypertrophy (RVHI%) in the Ctr, pulmonary arterial hypertension (PAH), adipose-derived stem cells (ADSCs), ADSCs-V and ADSCs-adiponectin (APN) groups. *P<0.05 vs. Ctr group; #P<0.05 vs. PAH group. (B) Pulmonary artery acceleration time (PAAT) by pulsed wave-Doppler echocardiography. Representative pulmonary artery flow in the short axis view at the level of the parasternal in the Ctr, PAH, ADSCs, ADSCs-V and ADSCs-APN groups.

expression in the PAH group was obviously higher than that in the Ctr group (Fig. 2D). After ADSCs and ADSCs-V treatments, slight suppression of α-SMA expression was found. Importantly, the α-SMA expression in the ADSCs-APN group was notably inhibited in comparison with the PAH, ADSCs and ADSCs-V groups. Thus, the increase in WT of pulmonary arterioles was positively associated with the enhancement of SMC proliferation. These results suggested that ADSCs-APN rather than ADSCs and ADSCs-V was able to powerfully reverse pulmonary vascular remodeling.

ADSCs-APN improve RV function. MCT treatment resulted in severe RV hypertrophy with a sharp increase in RVHI value as compared with the Ctr group (P<0.05) (Fig. 3A). There was no significant difference in the RVHI values between the PAH and ADSCs/ADSCs-V groups (P>0.05). However, compared to the PAH group, the RVHI value was significantly reduced by the ADSCs-APN transplantation (P<0.05).

Fig. 3B shows the pulmonary artery forward flow and the PAAT of rats after diverse treatments. In the Ctr group, the blood flow through pulmonary arteries had a typical 'rounded' shape. However, in the PAH group, the velocity profile of the pulmonary artery was altered to a 'spike and dome' morphology with reduced PAAT. After the ADSC and ADSCs-V treatments, the echo profiles showed that both PAAT and ejection time were obviously increased. Furthermore, this profile in the ADSCs-APN group was further improved and almost similar to the Ctr group with similar PAAT and morphology. It was suggested that ADSCs-APN rather than ADSCs and ADSCs-V vigorously attenuated the high resistance of the pulmonary artery.

The hemodynamic and structural characteristics including TAPSE, RVEDD, RVESD, RVWT and PAAT/HR measured by echocardiography are documented in Table I. TAPSE and PAAT/HR in the PAH group were significantly decreased as compared with the Ctr group (P<0.05), and this decrease was reversed to a relative high level in the ADSCs and ADSCs-V groups. ADSCs-APN further significantly raised the TAPSE and PAAT/HR as compared with the ADSCs and ADSCs-V groups (P<0.05). As for RVEDD, it was notably increased in the PAH group, and it was similar among the PAH, ADSCs, ADSCs-V and ADSCs-APN groups. RVESD and RVWT in the PAH group were significantly higher than those in the Ctr group (P<0.05), but after ADSCs, ADSCs-V and ADSCs-APN treatments, they were non-significantly reduced to relative low levels. There was no significant difference in all parameters between the ADSCs and ADSCs-V groups.

APN suppresses the proliferation of PASMCs via the AMPK/BMP/Smad signaling pathway. PAMSCs were isolated from the rats bearing PAH and they were presented as spindle shapes under phase contrast microscopy (Fig. 4A, left). The right image in Fig. 4A shows the immunofluorescence of PASMCs with α-SMA marking.

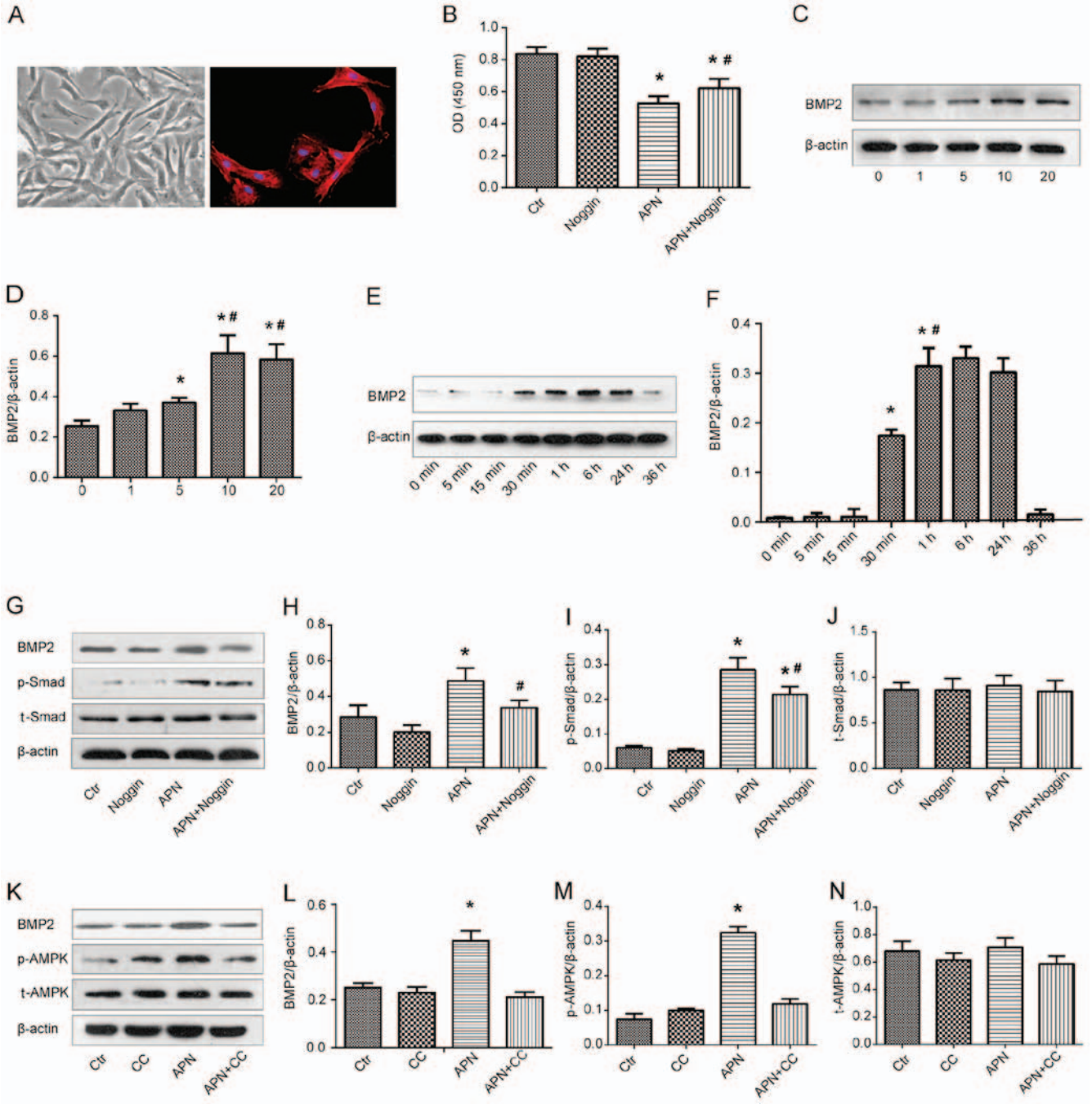

Figure 4. Effect of adiponectin (APN) on pulmonary artery smooth muscle cells (PASMCs). (A) Left, typical 'hill and valley' appearance of rat PASMCs under phase contrast microscope; right, positive immunofluorescent identification of α-smooth muscle actin (α-SMA). (B) Cell proliferation was analyzed by Cell Counting Kit-8 (CCK-8) assay. (C and D) PASMCs were incubated with APN (0-20 μg/ml) for 1 h and bone morphogenetic protein-2 (BMP2) expression was measured by western blot analysis. *P<0.05 vs. 0 μg/ml group; #P<0.05 vs. 5 μg/ml group. (E and F) PASMCs were incubated with 10 μg/ml APN for indicated time intervals and BMP2 expression was measured by western blot analysis. *P<0.05 vs. 0 min group; #P<0.05 vs. 30 min group. (G-N) Adiponectin (APN) exerted antiproliferative effects by modulating the AMPK/BMP/Smad signaling pathway. (G-J) Rat PASMCs were exposed to APN (10 μg/ml) and/or noggin (200 ng/ml) and BMP2, p-Smad and Smad expression was analyzed with western blot analysis. (K-N) PASMCs were treated with compound C (20 μmol/l) and/or APN (10 μg/ml) and BMP2, p-AMPK and AMPK expression was analyzed by western blot analysis. CC, Compound C. *P<0.05 vs. Ctr group; #P<0.05 vs. APN group.

PASMCs isolated from the rats with PAH were exposed to APN (10 μg/ml) and/or a specific BMP2 inhibitor noggin (200 ng/ml) and the viability of PASMCs was analyzed by CCK-8 assay (Fig. 4B). A similar absorbance was found between the Ctr and noggin groups. APN markedly reduced the absorbance as compared with the Ctr and noggin groups (P<0.05). However, after the combination treatment of APN and noggin, the absorbance was significantly reversed to a relative high level in comparison with the APN group (P<0.05). These results implied that APN inhibited the growth of PASMCs from the rats bearing PAH and that the inhibitory effect of APN was weakened by the BMP2 inhibitor.

The effect of APN on BMP2 protein expression was determined by qualitative and quantitative western blot analysis (Fig. 4C and D). The expression of BMP2 was upregulated along with the increase in the APN dosage (0, 1, 5 and

10 μg/ml), reaching a peak at 10 μg/ml of APN. There was no significant difference in the BMP2 expression between treatment with 10 and 20 μg/ml of APN. Therefore, the optimum dosage of APN was found to be 10 μg/ml. PASMCs were then incubated with APN (10 μg/ml) for varying time intervals and BMP2 protein expression was measured by western blot analysis again (Fig. 4E and F). APN elevated the expression of BMP2 in a time-dependent manner between 0 and 6 h and a peak value was found at 6 h. Next, it gradually decreased and returned to the baseline level at 36 h. These results indicated that APN upregulated the BMP2 protein expression in PAMSCs in dosage- and time-dependent manners.

In an attempt to identify the influence of APN on the BMP/Smad-related signaling pathways, the expression of BMP2, Smad, p-Smad, AMPK and p-AMPK after treatment with APN, noggin and CC was evaluated by western blot analysis (Fig. 4G-N). We found that APN treatment increased the expression of BMP2 and p-Smad proteins, while noggin downregulated their high expression levels induced by APN (Fig. 4G-I). Similarly, APN treatment elevated the expression of BMP2 and p-AMPK proteins, while CC downregulated their strong expression induced by APN (Fig. 4K-M). There was no difference in the expression of Smad and AMPK proteins among the above groups (Fig. 4J and N).

Discussion

PAH is a progressive disease characterized by increased pulmonary arterial pressure, pulmonary vascular remodeling, and RV dysfunction, which finally leads to right heart failure and death. The pathogenesis of PAH is still poorly understood, but it is intensely associated with excessively proliferative smooth muscle cells that disturb the balance among vasoactive substances and occlude the pulmonary arterial lumen (26). How to repair these damaged cells and restore their function are a major challenge for tissue regeneration engineering. In recent years, stem cells and cell-based gene therapy have become the most promising therapeutic strategies (27). Our results revealed that ADSCs were successfully isolated from rats and the APN gene was effectively transfected into the ADSCs. ADSCs were labeled with GFP to investigate the location of the ADSCs in the lung and we found that engrafted ADSCs in the lung were located around vessels. After the effective transplantation of ADSCs-APN into the rats presenting PAH, mPAP and RVHI were significantly decreased as compared with the ADSCs and ADSCs-V treatments. The WT of the small pulmonary arteries, which represents vascular remodeling, was also significantly reduced after ADSCs-APN treatment. Hyperplastic smooth muscle cells were evaluated by H&E and α-SMA immunohistochemical staining of tissue sections, and PAAT and echocardiographic parameters such as PAAT/HR, RVWT, RVESD, RVEED and TAPSE were more effectively improved by the ADSCs-APN treatment rather than ADSCs and ADSCs-V. These results suggest that antiproliferative activity plays a crucial role in the APN and ADSC combination therapy for PAH.

Many previous studies have investigated cell therapy such as EPCs and mesenchymal stromal cells for PAH (28,29). ADSCs are attractive cells for PAH therapy due to their easy achievement, low immunogenicity, multilineage differentiation potential, and abundant supply in the body. We found that ADSCs attenuated PAH and pulmonary arterial remodeling, which was in agreement with a previous study (30). ADSCs originate from adipose and have the ability to differentiate into vascular endothelial cells, vascular smooth muscle cells, and peripheral blood cells, thus promoting angiogenesis and graft survival (31). Moreover, ADSCs secrete a variety of cytokines and angiogenic factors to improve the tissue microenvironment (31,32). ADSCs also recruit host stem cells to the site of injury and activate the self-repair function (33).

However, other researchers have reported that ADSCs have no significant beneficial effect on MCT-induced PAH rats (6), which may be due to the differences in MCT dosage and administration method. In this study, we injected 40 mg/kg MCT to induce the PAH model and mPAP was elevated to ~33 mmHg, whereas the authors of the previous study administered 60 mg/kg MCT and mPAP reached up to 55 mmHg. It was possible that the higher pressure in the pulmonary artery largely weakened the positive effect of ADSC treatment. Moreover, we administrated ADSCs via the jugular vein, whereas they used intratracheal injections. Capillary beds are abundant in the lung tissues, which are beneficial for ADSC colonization. Therefore, it is speculated that intratracheal administration would not effectively improve the effect of ADSCs on PAH.

Increasing knowledge concerning the relationship between obesity and pulmonary vascular diseases has emerged. An autopsy study of 76 obese subjects revealed that the obese group had more extensive pulmonary hypertensive changes as compared with the control group (34). In addition, the REVEAL registry, the largest PAH database in the USA, indicated a higher prevalence of overweight and obese individuals among those with idiopathic forms of PAH (35). APN is one of the most important adipocytokines secreted from adipose tissue, which possesses biological pleiotropic actions in metabolism, immune regulation, and antiproliferative activities (36). APN may influence the progression of PAH. The WT of pulmonary vessels and RV hypertrophy were significantly increased and severe PAH was developed in the APN-deficient ($APN^{-/-}$) mice (14,15). APN overexpression was found to ameliorate pulmonary arterial remodeling and suppress elevated pulmonary artery pressure (17). In this study, after treatment with the ADSCs-APN, the hemodynamic changes and vascular remodeling of PAH were greatly attenuated. Furthermore, the combination of APN and ADSC therapy was much more effective than ADSC therapy alone.

To explore the underlying mechanisms in the PAH therapy here, we evaluated the thickness of the smooth muscle layer in the lung by examining the immunohistochemical expression of α-SMA. Compared to the Ctr group, all the treatment groups had a significantly smaller WT of pulmonary vasculature. The ADSCs-APN group had a thinner vascular wall than the ADSCs and ADSCs-V groups. It was suggested that APN attenuated the MCT-induced PAH and pulmonary arterial remodeling via ameliorating the wall thickening of the pulmonary arterioles. Moreover, APN was found to directly suppress the proliferation of PASMCs (25,37). The accumulation of smooth muscle cells in vessel walls was found to be enhanced and APN suppressed PAH by directly inhibiting PASMC proliferation in APN-deficient mice (14,15,17). Therefore, we hypothesized that the mechanism of reversing

vascular remodeling was associated with the anti-proliferation of PASMCs by APN and we probed the molecular mechanisms involved in this anti-proliferation process. It is well known that BMPs interact with receptors and trigger Smad phosphorylation to propagate the signals into the nucleus and regulate target gene expression (38). BMPs were found to inhibit the proliferation of smooth muscle cells through a Smad-dependent pathway (39,40). A dysfunctional BMP/Smad signaling pathway was found to be an important risk factor for hyperproliferative PASMCs (22,41-43). Therefore, we hypothesized that APN suppresses the proliferation of PASMCs via a BMP/Smad-dependent pathway.

In the present study, we found that APN partly reversed the defect of the BMP-stimulated Smad pathway in PASMCs with PAH. This indicated that the BMP/Smad signaling pathway plays a crucial part in the anti-proliferation of PASMCs by APN. The major downstream pathway of APN is the AMPK phosphorylation pathway. AMPK is not only involved in the regulation of glucose and lipid metabolism, but also has a variety of other biological activities, such as inhibition of tumor cell proliferation, autophagy, stress response and polarity regulation (44). Activation of AMPK was found to arrest the cell cycle in the G0/G1 phase and restrain tumor growth by increasing p53 expression (45). Additionally, AMPK activation may also suppress the proliferation of vascular smooth muscle cells via an mTOR-dependent pathway (46). Here, we demonstrated for the first time an involvement of the AMPK pathway in the BMP/Smad-dependent induction of proliferative inhibition by APN. Therefore, these results indicate that BMP/Smad may function as a downstream signaling pathway of AMPK in APN regulation. Taken together, our findings confirmed that APN suppressed PASMC proliferation via the AMPK/BMP/Smad pathway.

Besides the canonical BMP/Smad pathway, other non-Smad pathways such as MAPK kinases and PI3K kinase/Akt may also be involved in PAH pathogenesis (47-51). Here, we only evaluated the effect of APN on the Smad signaling pathway. It is yet unclear whether a non-Smad pathway is also involved in APN-mediated inhibition of PASMC proliferation and whether there is cross-talk between Smad and non-Smad pathways. This illustrates the complexity of understanding the BMP pathway and these issues will be investigated in our future studies.

We also confirmed that RV function was more effectively improved by ADSCs-APN transplantation rather than ADSC therapy alone. Although the observed beneficial effects of APN are incompletely understood, it is generally believed to exert its effects by decreasing oxidative stress of myocardial cells (52). Further studies are necessary to elucidate these gene-related mechanisms in myocardial cell lines.

In conclusion, transplantation of ADSCs attenuated MCT-induced PAH in rats, and transfection of APN into ADSCs further promoted this therapeutic effect *in vivo*. The main mechanism of this effect was that the anti-proliferation of PASMCs by APN based on the regulation of the AMPK/BMP/Smad pathway suppressed the hyperplasia of the pulmonary vascular wall. ADSCs are useful and effective vehicles with which to deliver therapeutic genes intravenously to the lung to treat PAH. At present, no effective therapeutic options are available for PAH. This study has important implications for PAH therapy and provides solid evidence to support future investigation of regenerative cell-based gene strategies for the treatment of patients with severe PAH and congenital heart disease. Therapies restoring APN signaling may present novel modalities to prevent PAH progression and its complications.

Acknowledgements

The authors are thankful for the financial support from the National Natural Science Foundation of China (nos. 81400189 and 81270111/H0109) and the Training Project for Young and Middle-Aged in the Health System of Fujian Province (no. 2013-ZQN-JC-21).

References

1. Liu K, Liu R, Cao G, Sun H, Wang X and Wu S: Adipose-derived stromal cell autologous transplantation ameliorates pulmonary arterial hypertension induced by shunt flow in rat models. Stem Cells Dev 20: 1001-1010, 2011.
2. Baber SR, Deng W, Master RG, Bunnell BA, Taylor BK, Murthy SN, Hyman AL and Kadowitz PJ: Intratracheal mesenchymal stem cell administration attenuates monocrotaline-induced pulmonary hypertension and endothelial dysfunction. Am J Physiol Heart Circ Physiol 292: H1120-H1128, 2007.
3. Zhao YD, Courtman DW, Deng Y, Kugathasan L, Zhang Q and Stewart DJ: Rescue of monocrotaline-induced pulmonary arterial hypertension using bone marrow-derived endothelial-like progenitor cells: Efficacy of combined cell and eNOS gene therapy in established disease. Circ Res 96: 442-450, 2005.
4. Luo L, Lin T, Zheng S, Xie Z, Chen M, Lian G, Xu C, Wang H and Xie L: Adipose-derived stem cells attenuate pulmonary arterial hypertension and ameliorate pulmonary arterial remodeling in monocrotaline-induced pulmonary hypertensive rats. Clin Exp Hypertens 37: 241-248, 2015.
5. Takemiya K, Kai H, Yasukawa H, Tahara N, Kato S and Imaizumi T: Mesenchymal stem cell-based prostacyclin synthase gene therapy for pulmonary hypertension rats. Basic Res Cardiol 105: 409-417, 2010.
6. Somanna NK, Wörner PM, Murthy SN, Pankey EA, Schächtele DJ, St Hilaire RC, Jansen D, Chaffin AE, Nossaman BD, Alt EU, *et al*: Intratracheal administration of cyclooxygenase-1-transduced adipose tissue-derived stem cells ameliorates monocrotaline-induced pulmonary hypertension in rats. Am J Physiol Heart Circ Physiol 307: H1187-H1195, 2014.
7. Zhao Q, Liu Z, Wang Z, Yang C, Liu J and Lu J: Effect of preprocalcitonin gene-related peptide-expressing endothelial progenitor cells on pulmonary hypertension. Ann Thorac Surg 84: 544-552, 2007.
8. Iwaguro H, Yamaguchi J, Kalka C, Murasawa S, Masuda H, Hayashi S, Silver M, Li T, Isner JM and Asahara T: Endothelial progenitor cell vascular endothelial growth factor gene transfer for vascular regeneration. Circulation 105: 732-738, 2002.
9. Cao G, Liu C, Wan Z, Liu K, Sun H, Sun X, Tang M, Bing W, Wu S, Pang X, *et al*: Combined hypoxia inducible factor-1α and homogeneous endothelial progenitor cell therapy attenuates shunt flow-induced pulmonary arterial hypertension in rabbits. J Thorac Cardiovasc Surg 150: 621-632, 2015.
10. Granton J, Langleben D, Kutryk MB, Camack N, Galipeau J, Courtman DW and Stewart DJ: Endothelial NO-synthase gene-enhanced progenitor cell therapy for pulmonary arterial hypertension: The PHACeT trial. Circ Res 117: 645-654, 2015.
11. Antonopoulos AS, Margaritis M, Coutinho P, Shirodaria C, Psarros C, Herdman L, Sanna F, De Silva R, Petrou M, Sayeed R, *et al*: Adiponectin as a link between type 2 diabetes and vascular NADPH oxidase activity in the human arterial wall: The regulatory role of perivascular adipose tissue. Diabetes 64: 2207-2219, 2015.
12. Lin Z, Pan X, Wu F, Ye D, Zhang Y, Wang Y, Jin L, Lian Q, Huang Y, Ding H, *et al*: Fibroblast growth factor 21 prevents atherosclerosis by suppression of hepatic sterol regulatory element-binding protein-2 and induction of adiponectin in mice. Circulation 131: 1861-1871, 2015.
13. Wang Y, Lam KS, Xu JY, Lu G, Xu LY, Cooper GJ and Xu A: Adiponectin inhibits cell proliferation by interacting with several growth factors in an oligomerization-dependent manner. J Biol Chem 280: 18341-18347, 2005.

14. Summer R, Fiack CA, Ikeda Y, Sato K, Dwyer D, Ouchi N, Fine A, Farber HW and Walsh K: Adiponectin deficiency: A model of pulmonary hypertension associated with pulmonary vascular disease. Am J Physiol Lung Cell Mol Physiol 297: L432-L438, 2009.
15. Medoff BD, Okamoto Y, Leyton P, Weng M, Sandall BP, Raher MJ, Kihara S, Bloch KD, Libby P and Luster AD: Adiponectin deficiency increases allergic airway inflammation and pulmonary vascular remodeling. Am J Respir Cell Mol Biol 41: 397-406, 2009.
16. Weng M, Baron DM, Bloch KD, Luster AD, Lee JJ and Medoff BD: Eosinophils are necessary for pulmonary arterial remodeling in a mouse model of eosinophilic inflammation-induced pulmonary hypertension. Am J Physiol Lung Cell Mol Physiol 301: L927-L936, 2011.
17. Nakagawa Y, Kishida K, Kihara S, Funahashi T and Shimomura I: Adiponectin ameliorates hypoxia-induced pulmonary arterial remodeling. Biochem Biophys Res Commun 382: 183-188, 2009.
18. Farber HW and Loscalzo J: Pulmonary arterial hypertension. N Engl J Med 351: 1655-1665, 2004.
19. Momose Y, Aimi Y, Hirayama T, Kataoka M, Ono M, Yoshino H, Satoh T and Gamou S: De novo mutations in the BMPR2 gene in patients with heritable pulmonary arterial hypertension. Ann Hum Genet 79: 85-91, 2015.
20. Soubrier F, Chung WK, Machado R, Grünig E, Aldred M, Geraci M, Loyd JE, Elliott CG, Trembath RC, Newman JH, *et al*: Genetics and genomics of pulmonary arterial hypertension. J Am Coll Cardiol 62 (Suppl 25): D13-D21, 2013.
21. Takahashi H, Goto N, Kojima Y, Tsuda Y, Morio Y, Muramatsu M and Fukuchi Y: Downregulation of type II bone morphogenetic protein receptor in hypoxic pulmonary hypertension. Am J Physiol Lung Cell Mol Physiol 290: L450-L458, 2006.
22. Upton PD and Morrell NW: The transforming growth factor-β-bone morphogenetic protein type signalling pathway in pulmonary vascular homeostasis and disease. Exp Physiol 98: 1262-1266, 2013.
23. Zhang S, Fantozzi I, Tigno DD, Yi ES, Platoshyn O, Thistlethwaite PA, Kriett JM, Yung G, Rubin LJ and Yuan JX: Bone morphogenetic proteins induce apoptosis in human pulmonary vascular smooth muscle cells. Am J Physiol Lung Cell Mol Physiol 285: L740-L754, 2003.
24. Xie L, Lin P, Xie H and Xu C: Effects of atorvastatin and losartan on monocrotaline-induced pulmonary artery remodeling in rats. Clin Exp Hypertens 32: 547-554, 2010.
25. Weng M, Raher MJ, Leyton P, Combs TP, Scherer PE, Bloch KD and Medoff BD: Adiponectin decreases pulmonary arterial remodeling in murine models of pulmonary hypertension. Am J Respir Cell Mol Biol 45: 340-347, 2011.
26. Rabinovitch M: Molecular pathogenesis of pulmonary arterial hypertension. J Clin Invest 122: 4306-4313, 2012.
27. Farkas L and Kolb M: Vascular repair and regeneration as a therapeutic target for pulmonary arterial hypertension. Respiration 85: 355-364, 2013.
28. Foster WS, Suen CM and Stewart DJ: Regenerative cell and tissue-based therapies for pulmonary arterial hypertension. Can J Cardiol 30: 1350-1360, 2014.
29. Suen CM, Mei SH, Kugathasan L and Stewart DJ: Targeted delivery of genes to endothelial cells and cell- and gene-based therapy in pulmonary vascular diseases. Compr Physiol 3: 1749-1779, 2013.
30. Eguchi M, Ikeda S, Kusumoto S, Sato D, Koide Y, Kawano H and Maemura K: Adipose-derived regenerative cell therapy inhibits the progression of monocrotaline-induced pulmonary hypertension in rats. Life Sci 118: 306-312, 2014.
31. Salgado AJ, Reis RL, Sousa NJ and Gimble JM: Adipose tissue derived stem cells secretome: Soluble factors and their roles in regenerative medicine. Curr Stem Cell Res Ther 5: 103-110, 2010.
32. Rehman J, Traktuev D, Li J, Merfeld-Clauss S, Temm-Grove CJ, Bovenkerk JE, Pell CL, Johnstone BH, Considine RV and March KL: Secretion of angiogenic and antiapoptotic factors by human adipose stromal cells. Circulation 109: 1292-1298, 2004.
33. Ii M, Horii M, Yokoyama A, Shoji T, Mifune Y, Kawamoto A, Asahi M and Asahara T: Synergistic effect of adipose-derived stem cell therapy and bone marrow progenitor recruitment in ischemic heart. Lab Invest 91: 539-552, 2011.
34. Haque AK, Gadre S, Taylor J, Haque SA, Freeman D and Duarte A: Pulmonary and cardiovascular complications of obesity: An autopsy study of 76 obese subjects. Arch Pathol Lab Med 132: 1397-1404, 2008.
35. Burger CD, Foreman AJ, Miller DP, Safford RE, McGoon MD and Badesch DB: Comparison of body habitus in patients with pulmonary arterial hypertension enrolled in the Registry to Evaluate Early and Long-term PAH Disease Management with normative values from the National Health and Nutrition Examination Survey. Mayo Clin Proc 86: 105-112, 2011.
36. Okamoto Y, Kihara S, Funahashi T, Matsuzawa Y and Libby P: Adiponectin: A key adipocytokine in metabolic syndrome. Clin Sci (Lond) 110: 267-278, 2006.
37. Wang ZV and Scherer PE: Adiponectin, cardiovascular function, and hypertension. Hypertension 51: 8-14, 2008.
38. García de Vinuesa A, Abdelilah-Seyfried S, Knaus P, Zwijsen A and Bailly S: BMP signaling in vascular biology and dysfunction. Cytokine Growth Factor Rev 27: 65-79, 2016.
39. Yang X, Long L, Southwood M, Rudarakanchana N, Upton PD, Jeffery TK, Atkinson C, Chen H, Trembath RC and Morrell NW: Dysfunctional Smad signaling contributes to abnormal smooth muscle cell proliferation in familial pulmonary arterial hypertension. Circ Res 96: 1053-1063, 2005.
40. Zeng Y, Liu H, Kang K, Wang Z, Hui G, Zhang X, Zhong J, Peng W, Ramchandran R, Raj JU, *et al*: Hypoxia inducible factor-1 mediates expression of miR-322: Potential role in proliferation and migration of pulmonary arterial smooth muscle cells. Sci Rep 5: 12098, 2015.
41. Morty RE, Nejman B, Kwapiszewska G, Hecker M, Zakrzewicz A, Kouri FM, Peters DM, Dumitrascu R, Seeger W, Knaus P, *et al*: Dysregulated bone morphogenetic protein signaling in monocrotaline-induced pulmonary arterial hypertension. Arterioscler Thromb Vasc Biol 27: 1072-1078, 2007.
42. Yang J, Li X, Al-Lamki RS, Wu C, Weiss A, Berk J, Schermuly RT and Morrell NW: Sildenafil potentiates bone morphogenetic protein signaling in pulmonary arterial smooth muscle cells and in experimental pulmonary hypertension. Arterioscler Thromb Vasc Biol 33: 34-42, 2013.
43. Yang J, Li X, Al-Lamki RS, Southwood M, Zhao J, Lever AM, Grimminger F, Schermuly RT and Morrell NW: Smad-dependent and smad-independent induction of id1 by prostacyclin analogues inhibits proliferation of pulmonary artery smooth muscle cells in vitro and in vivo. Circ Res 107: 252-262, 2010.
44. Vakana E, Altman JK and Platanias LC: Targeting AMPK in the treatment of malignancies. J Cell Biochem 113: 404-409, 2012.
45. Lévy J, Cacheux W, Bara MA, L'Hermitte A, Lepage P, Fraudeau M, Trentesaux C, Lemarchand J, Durand A, Crain AM, *et al*: Intestinal inhibition of Atg7 prevents tumour initiation through a microbiome-influenced immune response and suppresses tumour growth. Nat Cell Biol 17: 1062-1073, 2015.
46. Lee KY, Lee DH and Choi HC: Mesoglycan attenuates VSMC proliferation through activation of AMP-activated protein kinase and mTOR. Clin Hypertens 22: 2, 2016.
47. Lu J, Shimpo H, Shimamoto A, Chong AJ, Hampton CR, Spring DJ, Yada M, Takao M, Onoda K, Yada I, *et al*: Specific inhibition of p38 mitogen-activated protein kinase with FR167653 attenuates vascular proliferation in monocrotaline-induced pulmonary hypertension in rats. J Thorac Cardiovasc Surg 128: 850-859, 2004.
48. Ma J, Zhang L, Han W, Shen T, Ma C, Liu Y, Nie X, Liu M, Ran Y and Zhu D: Activation of JNK/c-Jun is required for the proliferation, survival, and angiogenesis induced by EET in pulmonary artery endothelial cells. J Lipid Res 53: 1093-1105, 2012.
49. Yu MQ, Liu XS, Wu HX, Xiang M and Xu YJ: ERK1/2 promotes cigarette smoke-induced rat pulmonary artery smooth muscle cells proliferation and pulmonary vascular remodeling via up-regulating cycline1 expression. J Huazhong Univ Sci Technolog Med Sci 33: 315-322, 2013.
50. Chen XY, Dun JN, Miao QF and Zhang YJ: Fasudil hydrochloride hydrate, a Rho-kinase inhibitor, suppresses 5-hydroxytryptamine-induced pulmonary artery smooth muscle cell proliferation via JNK and ERK1/2 pathway. Pharmacology 83: 67-79, 2009.
51. Havrda MC, Johnson MJ, O'Neill CF and Liaw L: A novel mechanism of transcriptional repression of p27kip1 through Notch/HRT2 signaling in vascular smooth muscle cells. Thromb Haemost 96: 361-370, 2006.
52. Guo Z, Qi W, Yu Y, Du S, Wu J and Liu J: Effect of exenatide on the cardiac expression of adiponectin receptor 1 and NADPH oxidase subunits and heart function in streptozotocin-induced diabetic rats. Diabetol Metab Syndr 6: 29, 2014.